Validation of a Low-cost Inertial Exercise Tracker

Sarvenaz Salehi[1] and Didier Stricker[2]
[1]*Daimler Protics, Germany*
[2]*German Research Center for Artificial Intelligence (DFKI), Germany*

Keywords: Inertial Sensors, Body-IMU Calibration, Body Motion Tracking, Exercise Monitoring.

Abstract: This work validates the application of a low-cost inertial tracking suit, for strength exercise monitoring. The procedure includes an offline processing for body-IMU calibration and an online tracking and identification of lower body motion. We proposed an optimal movement pattern for the body-IMU calibration method from our previous work. Here, in order to reproduce real extreme situations, the focus is on the movements with high acceleration. For such movements, an optimal orientation tracking approach is introduced, which requires no accelerometer measurements and it thus minimizes error due to outliers. The online tracking algorithm is based on an extended Kalman filter(EKF), which estimates the position of upper and lower legs, along with hip and knee joint angles. This method applies the estimated values in the calibration process i.e. joint axes and positions, as well as biomechanical constraints of lower body. Therefore it requires no aiding sensors such as magnetometer. The algorithm is evaluated using optical tracker for two types of exercises: squat and hip abd/adduction which resulted average root mean square error(RMSE) of 9cm. Additionally, this work presents a personalized exercise identification approach, where an online template matching algorithm is applied and optimised using zero velocity crossing(ZVC) for feature extraction. This results reducing the execution time to 93% and improving the accuracy up to 33%.

1 INTRODUCTION

Strength training is one of the critical components of the most fitness and rehabilitation processes. Monitoring such exercises is beneficial, in terms of performance improvement, injury prevention and rehabilitation(Bleser et al., 2015).

Wearable systems, including multiple sensors such as inertial measurement units(IMUs), provide an efficient solution for such applications. The kinematics analysis of body movements can be performed by fusing and filtering the well calibrated IMU measurements and extracting higher level information, such as joint angles and the segment positions (Yan et al., 2017; Chardonnens et al., 2013). In the previous work (Salehi et al., 2014), we presented the design and development of a low-cost tracking suit which composed of a wired network of IMUs and can be used for a long time exercise monitoring. In the current work the system is validated by a sequence of processes including body-IMU calibration, body pose estimation and personalized exercise identification, in order to provide a complete monitoring of user's performance.

2 RELATED WORKS

2.1 Body-IMU Calibration

Body-IMU calibration is a key requirement for capturing accurate body movements in applications based on wearable systems (Zinnen et al., 2009). The mounting positions of IMU with respect to joint is critical information in joint angle estimation using accelerometer measurements, especially during fast rotations (Cheng and Oelmann, 2010) and when modelling kinematic chains (Reiss et al., 2010). To obtain such values from manual measurements or anthropometric tables for different types of users is highly error-prone and cumbersome. We previously proposed a practical auto-calibration method for IMU to body position estimation in (Salehi et al., 2015), based upon a previously existing method by (Seel et al., 2014). In contrast to (Seel et al., 2014), our method considers three linked segments with IMUs (pelvis, upper leg, lower leg) and, respectively, two joints (hip, knee) in one estimation problem. This makes it possible to benefit from an additional constraint, which has shown theoretically and experimen-

Salehi, S. and Stricker, D.
Validation of a Low-cost Inertial Exercise Tracker.
DOI: 10.5220/0008965800970104
In *Proceedings of the 9th International Conference on Sensor Networks (SENSORNETS 2020)*, pages 97-104
ISBN: 978-989-758-403-9; ISSN: 2184-4380

tally to provide more robust and accurate results under suboptimal movement conditions. However, in experiments with real data the dependency to global IMU orientation could degrade the results due to magnetic disturbances and outliers in accelerometer measurements. In the current work the algorithm is evaluated using data from two different types of movements. In order to minimize the error due to existing outliers, especially in high acceleration, an optimal orientation tracking algorithm is proposed, which estimates relative rotations of the segments using gyroscope measurements. Therefore, the system is validated by this process, considering its applicability for different types of users, who perform the movements with different intensities and mostly with high acceleration.

2.2 Body Pose Estimation

In order to provide higher-level information such as body segments positions and joint angles, as well as 3D visualization of the movements in the targeted exercise monitoring application, a variety of techniques are proposed in the literature. Commonly, they assume the body segments to be rigid bodies, which are connected at joints.

A real-time motion tracking system was presented in (Zhu and Zhou, 2004), using a linear Kalman filter; the orientation of each body segment is calculated using accelerometer and magnetometer measurements and fused with gyroscope measurements in the Kalman filter, which results a smooth estimation. This approach, however, doesn't assume the error caused by linear acceleration in accelerometer measurement. Moreover, the magnetic disturbances are not modelled. This could lead to faulty estimation in the vicinity of ferromagnetic materials.

In order to consider the error of linear acceleration, the idea of using physical and virtual sensor, based on Newton-Euler equations, for estimating joint angle is presented in (Dejnabadi et al., 2006). According to this method, acceleration of the joint can be measured by placing a pair of virtual sensors on the adjacent links at the joint center. In these approaches, joint angle is defined by the difference of direction in measured acceleration of sensors in the joint frame. (Cheng and Oelmann, 2010) provides a survey, which compares four different methods for measuring the joint angle in two dimensions. They proved that when the sensors are mounted far from the joint center, especially in fast rotations a method called CMRGD: common-mode-rejection with gyro differentiation has less error and is easier to implement than the other methods. In this method, the gyroscope measurements are numerically differentiated in order to derive the angular acceleration, which is required to calculate the acceleration vector of the joint center.

Instead of using the magnetometer measurements, as they can easily distort the orientation estimation, different studies applied the biomechanical constraints in order to improve the estimation of body motion in the horizontal plane. Such studies can be divided into two categories:
In the first category, the joint angles are estimated in an state estimation approach, assuming the known IMUs mounting orientations. In (Lin and Kulić, 2012), with the assumption of constant joint acceleration and using Denavit-Hartenberg (DH) convention, the angle related to each possible degree of freedom(DOF) at hip and knee joints is estimated in an EKF. Here the accelerometer measurement model follows a similar approach in (Cheng and Oelmann, 2010) and (Dejnabadi et al., 2006).
In the second category, the state vector contains the relative orientation and the position of the segments. In (Kok et al., 2014), an optimization approach incorporates the biomechanical constraints together with the biases of inertial sensors and the error of limited DOF on knee joint. Other than body pose, the body-IMU calibration parameters are simultaneously estimated. However, (Kok et al., 2014) didn't present any evaluation of accuracy of such parameters. Moreover, this approach can not be used in a real-time application, as it requires a batch of observations.
In the same category of methods, (Luinge et al., 2011) proposed the Kinematic Coupling(KiC) algorithm, at first for a hinge joint; Assuming A and B are IMUs, which are mounted on the adjacent segments of the joint m, from the coupling concept the following constraint is defined:

$$^{G}\Delta\vec{P} = {}^{G}\vec{l}mB - {}^{G}\vec{l}mA \quad (1)$$

,where $^{G}\Delta\vec{P}$ is the relative position of B wrt. A and $^{G}\vec{l}mA$,$^{G}\vec{l}mB$ are the distance vector between joint m and the respective IMUs, all defined in the global coordinate system, G, which is typically aligned with gravity and magnetic north. In this case the EKF state vector contains relative positions and velocities of two adjacent segments of the joint, the error in orientation of the segments and gyroscope biases. In this work we propose a similar approach to (Luinge et al., 2011), in order to estimate the relative velocity and position of a leg segments, in addition to hip and knee joint angles. Using the biomechanical constraints and result of body-IMU calibration, the number of required states is less in comparison to (Luinge et al., 2011), plus there's no need for extra measurements, such as magnetic field.

2.3 Exercise Identification

It is common that trainers initially monitor trainees and instruct them based on their health conditions, while they are performing a strength exercise for the first time, so that they can independently perform the exercise later. Possibility of injuries are normally high in this phase, as the correct way of the exercise can't be carefully controlled, considering body characteristics and abilities of individuals. For example, in the rehabilitation, where range of motion is limited in different stages of recovery. It is thus very important to provide a personalized monitoring application.

Exercise identification is the process of identifying the start and stop time of one repetition in an exercise, which could be composed of multiple smaller components known as motion primitives. Usually a repetition in an strength exercise comprises the sequence of increasing and decreasing velocity. Therefore, zero velocity crossing(ZVC) approach is one of the most optimal approaches to find the motion primitives, where the velocity of signal changes the sign. (Fod et al., 2002) applied ZVCs, in order to detect the motion primitive of two DOFs.

Hidden Markov Model(HMM) is a stochastic approach, which considers a signal as unobservable sequences of Markov states. At each time point the system undergoes a state transition, which is defined by a probability in a transition matrix. In (Janus and Nakamura, 2005), a template free approach is proposed, where the data is windowed and probability density function of each window was used in a HMM to detect different states of the movements. The segment is identified, where the transition between states occurs.

HMM is more used in the template based approaches. In (Lin and Kulić, 2013) a two-stage approach is proposed to reduce the computational cost by reducing the number of times that HMM should run. This is achieved by first scanning the observation signal for the candidate segments using ZVC or velocity peaks in joint angle.

There are other learning based classifiers, which are used for motion identification such as Convolutional Neural Network(CNN) (Um et al., 2017) or Support Vector Machine(SVM) (Morris et al., 2014). However, they require enough labelled training data to increase the accuracy.

An alternative approach, which doesn't require any training data is template matching.

Dynamic Time Warping(DTW) is a popular template matching algorithm, which creates a matrix of the distances between each point of the observed signal and the template. Then this matrix is searched for a warping path which leads to a minimum distance. This can be used to identify an exercise using a template of motion data, performed and captured with the supervision of a trainer. However, it can be only applied in offline scenarios, due to its expensive computational cost, especially in higher dimensions. (Sakurai et al., 2007) proposed an online approach, which addresses the problem of subsequent matching using DTW. This algorithm is fast which means the processing time of current observation point doesn't depend on the past data length. It only requires a single matrix to find the matching subsequent. In (Sakurai et al., 2007), an experiment on joint position data from optical motion capture system is presented. Here, this algorithm was evaluated for real time motion identification based on IMU measurements.

3 PROCEDURE

3.1 Body-IMU Calibration

The calibration procedure is based on the method in (Salehi et al., 2015), here using two different types of movements: A) random movements in all directions, B)separate movements on each DOF. Additionally, in order to avoid problems such as outlier and distorted measurements, caused when using accelerometer and magnetometer, a new approach is proposed, specifically for movements of type B, in order to estimate the relative orientations, which are required for calibration procedure (see Figure 1). This is explained in the following section:

3.1.1 Relative Orientation Estimation

Considering a hinge joint, n, the measurements of gyroscopes ($\vec{\omega}$), mounted on its two adjacent segments (B,C), provide useful information in order to identify the joint axis $\vec{r}_n$. As the rotation is limited to only one direction i.e. joint axis, any difference between the angular velocities of the two segments, in the plane perpendicular to the rotation, is in contrast to that limited degree of freedom. It is also obvious that the difference between the angular velocities of the segments in the direction of the joint axis is the joint angular velocity. These facts are defined in the equations 2 and 3.

$$\|\vec{\omega}_B \times {}^B\vec{r}_n\| - \|\vec{\omega}_C \times {}^C\vec{r}_n\| = 0 \tag{2}$$

$$\dot{\theta}_n = \omega_B \cdot {}^B\vec{r}_n - \omega_C \cdot {}^C\vec{r}_n \tag{3}$$

,where $\cdot$ is scalar product. Thus the joint axis can be estimated, using a set of measurements from two gyroscopes on the joint segments, in an optimization

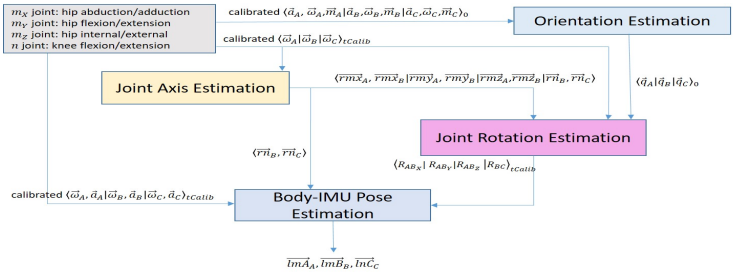

Figure 1: The computation graph of body-IMU calibration procedure.

problem, with equation 2 as the cost function. The relative segment orientation is obtained from integration of equation 3. Though this approach is explained for knee joint, the same can be applied for hip, if the movements are kept limited to only one DOF at a time (see Figure 1). Therefore type B movements provides optimal measurements for both joint axes and relative orientation estimation, which are the prerequisites for body-IMU calibration algorithm.

3.2 Body Pose Estimation

In this work an extended Kalman filter is designed to estimate the knee and hip joint angles, as well as the legs' segments positions. The assumptions here are: (1) a simple biomechanical model for leg with rigid segments connected via frictionless joints: hip(m), knee(n), (2) at least one IMU sitting on each rigid segment that should be tracked: (A on pelvis, B on upper leg, C on lower leg), (3) forward kinematics equations, (4) constant acceleration for integration duration(sampling time).

The state vector, Equation 4, includes the velocities($\vec{v}$) and positions($\vec{P}$) of the upper and lower segments in addition to the hip rotation quaternion($\vec{q}_{AB}$), and the knee joint angle($\vec{\theta}_{BC}$), all of which are wrt pelvis coordinate:

$$\vec{x} = [{}^A\vec{v}_B \quad {}^A\vec{v}_C \quad {}^A\vec{P}_B \quad {}^A\vec{P}_C \quad \vec{q}_{AB} \quad \vec{\theta}_{BC}] \tag{4}$$

Kinematic Process Model is defined in Equation 5 (note: tilde superscripts indicate the measurements and the vector signs is removed for simplicity).

$$ {}^A v_{B_k} = {}^A v_{B_{k-1}} + {}^A \tilde{a}_{B_{k-1}} \Delta T \tag{5a}$$
$$ {}^A v_{C_k} = {}^A v_{C_{k-1}} + {}^A \tilde{a}_{C_{k-1}} \Delta T \tag{5b}$$
$$ {}^A P_{B_k} = {}^A P_{B_{k-1}} + {}^A v_{B_{k-1}} \Delta T + \frac{{}^A \tilde{a}_{B_{k-1}} \Delta T^2}{2} \tag{5c}$$
$$ {}^A P_{C_k} = {}^A P_{C_{k-1}} + \Delta T {}^A v_{C_{k-1}} + \frac{{}^A \tilde{a}_{C_{k-1}} \Delta T^2}{2} \tag{5d}$$
$$ q_{AB_k} = exp(R_{AB_{k-1}} \tilde{\omega}_{B_{k-1}} - \tilde{\omega}_{A_{k-1}}) q_{AB_{k-1}} \tag{5e}$$
$$ \theta_{BC_k} = \theta_{BC_{k-1}} + \Delta T (\tilde{\omega}_{C_{k-1}} \cdot {}^C r_n - \tilde{\omega}_{B_{k-1}} \cdot {}^B r_n) \tag{5f}$$

,where

$$ {}^A \tilde{a}_{B_{k-1}} = R_{AB_{k-1}} \tilde{a}_{B_{k-1}} - \tilde{a}_{A_{k-1}} \tag{6a}$$
$$ {}^A \tilde{a}_{C_{k-1}} = R_{AB_{k-1}} R_{BC_{k-1}} \tilde{a}_{C_{k-1}} - \tilde{a}_{A_{k-1}} \tag{6b}$$

Here, accelerometer($\tilde{a}$) and gyroscope($\tilde{\omega}$) measurements are the control inputs. R_{AB} is obtained from q_{AB} using the quaternion to rotation matrix conversion and R_{BC} is calculated from $\vec{\theta}_{BC}$ and ${}^B r_n$ using the axis-angle to rotation matrix conversion. ΔT is the sampling time.

Observation Model is defined based on assumption 1; the segments pelvis and upper leg connected in hip joint (Equation 7a) and upper and lower legs connected in knee joint (Equation 7b):

$$ P_{B_k} = -R_{AB}{}^B lmB + {}^A lmA \tag{7a}$$
$$ P_{C_k} = -R_{AB}(R_{BC}{}^C lmC + {}^B lmB) + {}^A lmA, \tag{7b}$$

3.3 Exercise Identification

In this work a template based exercise identification algorithm is proposed, which deploys the recorded supervised exercise motion as the template for later identification of correct performance. Here, we applied a streaming subsequence matching method, SPRING (Sakurai et al., 2007). For further optimization of execution time, a preprocessing stage, including motion primitive detection and a feature extraction step, are presented in this section.

3.4 Preprocessing

3.4.1 Motion Primitive Detection

As the strength exercises mostly contain the periodic pattern, where the velocity of motion increases and decreases sequentially, we chose ZVC method to detect the motion primitives in the template as well as in the streaming signal. Therefore the motion primitive is detected, where the sign of derivative is changing on the dominant DOF of motion signals e.g. positions or joint angles. The derivative is calculated here using a sliding window of 3 samples. The dominant DOF

is selected on each dataset by finding a dimension of template signal which has the highest value.

3.4.2 Feature Extraction

The features consist of velocity, variance and mean of each DOF in motion primitive. Therefore, for each motion primitive tens of input samples are reduced to 3 features for each dimension. This, as it is shown in the experimental results, has increased the speed of identification.

4 EXPERIMENTAL RESULTS

4.1 Body-IMU Calibration

In order to evaluate the proposed method, we captured a dataset from 7 subjects, 2 women and 5 men, each performing 3 trials using the IMU harness of the tracking suit, presented in (Salehi et al., 2014), and an optical reference system, the NaturalPoint OptiTrack, with 12 Prime 13 cameras, operated with the Motive software (Optitrack, 2019). The test setup is shown in Figure 2. In this experiment, each IMU was rigidly connected with a rigid body marker. The IMUs were interconnected via textile cables. In order to reduce artefacts due to movement of the garment, the IMU-marker-sets were strapped firmly on the pelvis and one leg. We also used straps in order to attach marker clusters on anatomical landmarks around the hip and knee joints, from which we determined the joint center of rotations.

In each trial, the subjects performed movements of type A and B. In order to assess the repeatability of the process each subject has done three trials. Data in both optical system and IMUs captured with $50Hz$ rate. The IMU measurements then were downsampled to $5Hz$. A hand-eye calibration was used to transform the optical system coordinate to the IMU coordinates. Note that errors due to marker positioning are present, however, similarly for all the tested methods. The data from type B movements was first used to estimate the joints' axes, by applying method described in 3.1.1. The calibration algorithms were applied to both types of data. The following describes the preprocessing and result analysis of each one:

A. Calibration with Random Movements in All Directions. For this type of movements, the global IMU orientations were calculated based on a similar approach in (Harada et al., 2007), using IMU measurements.

Figure 2: The red arrows show three IMUs which are mounted on 1.pelvis (not visible), 2.upper leg and 3.lower leg.

Figure 3 illustrates the overall RMSE in all the four segments for all the trials, when applying the different calibration methods. This shows that the proposed method provides more accurate results in 80% of the trials, while a slightly worse performance can be observed in the rest. The average error over all the trials in the proposed method is $16.9\pm0.8cm$, which is lower than the ones of the Seel *et al.* method with error of $18.13\pm0.7cm$. The more detailed result of proposed method is presented in Table 1. It can be observed that the errors in segments lmA and lmB are higher than the ones in lnB and lnC, as the movements of these segments around the hip joint are more limited than the ones around the knee. This was also proved theoretically, in the observability analysis in (Salehi et al., 2015): conditions 2 and 3, which are related to the angular velocity variations.

B. Calibration with Separate Movements on Each DOF Both approaches are applied on the dataset, which includes separate movements in each DOF. Here, in order to estimate the relative orientations of the segments, we applied the method in 3.1.1. Figure 4 illustrates the overall RMSE in all the four segments for all the trials, which shows the proposed method has more accurate results in all the trials with the average error of $15.1\pm0.6cm$. The detailed result of proposed method in Table 1.

It is shown that the proposed method with the dataset of type B movements results better than the type A, while the Seel *et al.* method results worse. This proves the first condition of observability in (Salehi et al., 2015). Moreover, during the experiment with the random movements in order to excite all the segments simultaneously the subjects have performed fast and hardly controlled movements, which led to high deviation of accelerometer measurements

Table 1: The positions of each joint m,n with respect to each IMU A,B,C estimated by method in (Salehi et al., 2015) from 7 subjects performing type A movements.

cm	s1	s2	s3	s4	s5	s6	s7
lmA	12.5±3.37	18.57±4.3	15.6±1.19	15.99±2.14	15.02±3.31	16.89±0.7	13.68±5.1
lmB	24.39±0.9	22.28±4.93	19.72±2.58	23.34±2.81	25.92±3.97	24.8±3.16	31.18±3.79
lnB	9.98 ±6.37	16.12±0.52	10.26±3.33	9.35±2.01	12.49±4.62	10.12±1.85	7.23±3.87
lnC	14.86±0.47	12.85±1.57	9.5±1.34	9.48±1.15	11.54±2.86	15.24±5.94	11.86±5.23

Table 2: The positions of each joint m,n with respect to each IMU A,B,C estimated by method in (Salehi et al., 2015) and Section 3.1.1 from 7 subjects performing type B movements.

cm	s1	s2	s3	s4	5	s6	s7
lmA	23.13±3.26	18.18±3.53	14.12±1.69	14±3.07	13.51±4.07	17.33±0.82	15.2±0.73
lmB	14.26±0.87	17.03±4.98	19.69±3.04	18.42±2.88	16.49±7.61	20.21±2.23	24.79±4.37
lnB	13.5±4.93	14.66±3.5	7.86±1.55	6.4±2.65	13.89±5.54	8.2±1.88	3.61±1.92
lnC	13.72±0.22	11.71±3.23	9.93±0.93	10.17±2.51	8.88±5.49	13.34±3.14	11.94±3.86

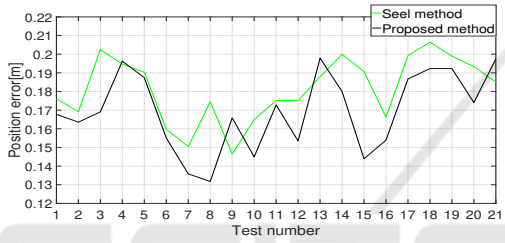

Figure 3: Results on measurements from random movements: RMSE of the body-IMU calibration using Seel *et al.*(green) and the proposed method(black), with respect to optical tracker. Test 1,2,3 is with subject 1, test 4,5,6 with subject 2, etc.

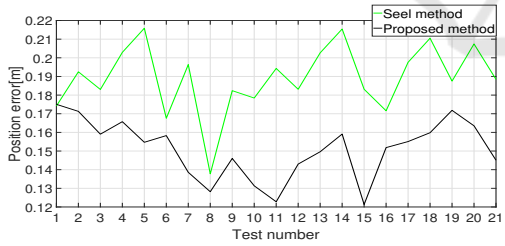

Figure 4: Results on measurements from the movements on each DOF separately: RMSE of the Body-IMU calibration using Seel *et al.*(green) and the proposed method(black), with respect to optical tracker.

from gravity. Commonly in most of the orientation estimation filters, these measurements are considered as outliers and the estimated orientation in the presence of such measurements is prone to error. This has led to higher error in the proposed method than when using type B measurements.

Table 3: Error of estimated upper and lower segments positions using the proposed method for squat exercise.

cm	PB [RMS, STD, Max]	PC [RMS, STD, Max]
s1	[8.47, 10.02, 4.10]	[8.98, 8.43, 36.16]
s2	[7.72, 5.13, 16.53]	[7.69, 3.87, 14.20]
s3	[6.05, 4.44, 15.30]	[9.12 5.49, 17.68]
s4	[6.57, 4.93, 19.92]	[7.51, 6.14, 24.64]
s5	[8.91, 5.10, 18.02]	[7.84, 4.14, 16.96]
s6	[7.20, 4.03, 13.73]	[5.47, 3.55, 12.84]
s7	[6.40, 4.65, 15.27]	[7.42, 5.15, 18.53]

Table 4: Error of estimated upper and lower segments positions using the proposed method for abduction and adduction exercise.

cm	PB [RMS, STD, Max]	PC [RMS, STD, Max]
s1	[5.19, 3.38, 10.57]	[10.53, 6.91, 21.40]
s2	[4.83, 2.97, 25.61]	[9.96, 6.14, 24.84]
s3	[4.60, 1.99, 8.52]	[10.63, 5.66, 21.18]
s4	[7.16, 3.87, 13.84]	[12.31, 7.14, 24.65]
s5	[6.10, 3.64, 12.40]	[12.43, 8.58, 27.58]
s6	[7.74, 4.58, 15.56]	[16.28, 11.0, 34.62]
s7	[8.09, 5.95, 19.45]	[16.33, 12.84, 42.45]

4.2 Lower Body Pose Estimation

The pose estimation approach in Section 3.2 was evaluated for lower body movements. The state vector is initialized using the Equations 7a and 7b. The initial global orientations and pelvis orientation were estimated using a similar approach to in (Harada et al., 2007). With the setup similar to Section 4.1, estimation of a leg segments positions captured by both

Table 5: Joint angle identification without ZVC.

	s1	s2	s3	s4	s5	s6	s7
Accuracy[%]	99	99	99	99	99	99	99
Precision[%]	100	100	100	100	100	100	100
Time[s]	4.4	3.1	3.0	2.1	2.8	4.5	2.7

Table 6: Joint angle identification with ZVC.

	s1	s2	s3	s4	s5	s6	s7
Accuracy[%]	99	77	99	99	98	99	98
Precision[%]	100	6	100	71	100	80	40
Time[s]	0.4	0.2	0.2	0.1	0.1	0.1	0.2

tracking suit and optical system. This experiment was carried out with 7 subjects each performing squat and hip abduction/adduction exercises.

The results for squat and abduction/adduction exercises are presented in Tables 3 and 4 respectively. The average error for all subjects in estimation of lower leg position, is higher than upper leg, as it contains more error related to knee joint angle plus the calibration error of IMU position in particular lnC.

4.3 Exercise Monitoring

The algorithm was evaluated using the result of body motion tracking in section 4.2. The first squat which was performed following the instruction of a supervisor, was used as a template to identify the next repetitions. After squats the subjects have performed other movements, Figure 5.

As the joint angle is commonly used in the movement identification, here this signal was used as a baseline to evaluate the exercise identification for when using ZVC for feature extraction. As it can be seen from Tables 5 and 6, applying ZVC has a high impact on the execution time.

For position signal, the average accuracy and precision are higher than these values for the joint angles. This implies that the position signals in comparison to the joint angles, contain more information related to type of exercise. For more detailed comparison see Tables 6,7.

The last experiment was done by using the pelvis orientation as an additional input, as the correct performance of the squat exercise is highly depends the pelvis movements. The result is presented in Table 8. It was noticed that in only one test, where the subject didn't follow the instructed exercise, the sensitivity is lower in comparison to the previous experiment.

Table 7: Position identification with ZVC.

	s1	s2	s3	s4	s5	s6	s7
Accuracy[%]	99	99	99	98	98	99	99
Precision[%]	100	83	100	100	100	100	100
Sensitivity[%]	25	100	60	20	28	20	20
Time[s]	0.6	0.2	0.1	0.1	0.1	0.2	0.1

Table 8: Position plus quaternion identification with ZVC.

	s1	s2	s3	s4	s5	s6	s7
Accuracy[%]	99	99	99	98	98	99	99
Precision[%]	100	83	100	100	100	100	100
Sensitivity[%]	25	100	60	20	14	20	20
Time[s]	0.9	0.3	0.2	0.1	0.1	0.2	0.2

5 CONCLUSIONS

In this work the application of exercise monitoring is presented in order to validate a low-cost inertial tracking suit. This has been achieved following three different processes: offline body-IMU calibration, online body pose estimation and online exercise identification. It was shown that using the previous body-IMU calibration method for random movements, degrade the results due to the presence of outliers especially from accelerometer measurements. Therefore an optimal orientation tracking method was proposed, which can be realized using only gyroscope measurements, while the user performs separate movements around each DOF. Using dataset from this type of movements, the result showed overall improvement, especially for the leg segments, which can not provide enough useful movements for calibration. The body pose estimation approach is based on EKF, where only inertial measurements are contributing as control inputs. In the proposed approach the lack of a reliable reference measurement for the horizontal plane,

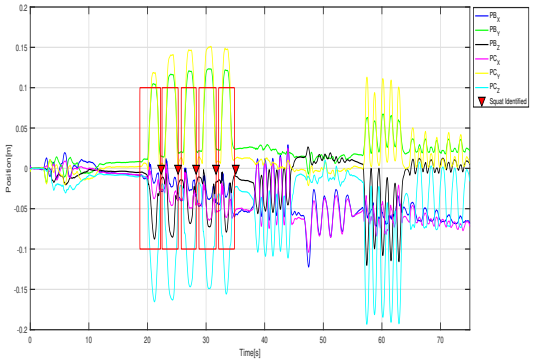

Figure 5: Online squat exercise identification. The red arrows show the timestamps when the squats are identified.

e.g. magnetic field, was compensated by modelling the joints' constraints in observation model and using the body-IMU calibration results, i.e. joint axes and positions. In order to monitor the strength exercises, a personalized identification approach was proposed, which doesn't require a large labelled training dataset. The idea is to use a template signal captured, where users are instructed to perform the movements correctly according to their ability and health conditions. Therefore, an online template matching algorithm is optimized and applied to estimated position, which led to improved accuracy and execution time. The experimental results of this validation showed relatively good results, considering high intensity of the movements. For further improvement in future , in order to compensate for the intensive dynamic movements, an outlier rejection approach can be implemented. Additionally performance of EKF can be improved by adaptive tuning of the noise covariances.

REFERENCES

Bleser, G., Steffen, D., Reiss, A., Weber, M., Hendeby, G., and Fradet, L. (2015). Personalized physical activity monitoring using wearable sensors. In *Smart health*, pages 99–124. Springer.

Chardonnens, J., Favre, J., Cuendet, F., Gremion, G., and Aminian, K. (2013). A system to measure the kinematics during the entire ski jump sequence using inertial sensors. *Journal of biomechanics*, 46(1):56–62.

Cheng, P. and Oelmann, B. (2010). Joint-angle measurement using accelerometers and gyroscopes?a survey. *IEEE Transactions on instrumentation and measurement*, 59(2):404–414.

Dejnabadi, H., Jolles, B. M., Casanova, E., Fua, P., and Aminian, K. (2006). Estimation and visualization of sagittal kinematics of lower limbs orientation using body-fixed sensors. *IEEE Transactions on Biomedical Engineering*, 53(7):1385–1393.

Fod, A., Matarić, M. J., and Jenkins, O. C. (2002). Automated derivation of primitives for movement classification. *Autonomous robots*, 12(1):39–54.

Harada, T., Mori, T., and Sato, T. (2007). Development of a tiny orientation estimation device to operate under motion and magnetic disturbance. *The International Journal of Robotics Research*, 26(6):547–559.

Janus, B. and Nakamura, Y. (2005). Unsupervised probabilistic segmentation of motion data for mimesis modeling. In *ICAR'05. Proceedings., 12th International Conference on Advanced Robotics, 2005.*, pages 411–417. IEEE.

Kok, M., Hol, J. D., and Schön, T. B. (2014). An optimization-based approach to human body motion capture using inertial sensors. *IFAC Proceedings Volumes*, 47(3):79–85.

Lin, J. F. and Kulić, D. (2012). Human pose recovery using wireless inertial measurement units. *Physiological measurement*, 33(12):2099.

Lin, J. F.-S. and Kulić, D. (2013). Online segmentation of human motion for automated rehabilitation exercise analysis. *IEEE Transactions on Neural Systems and Rehabilitation Engineering*, 22(1):168–180.

Luinge, H. J., Roetenberg, D., and Slycke, P. J. (2011). Inertial sensor kinematic coupling. US Patent App. 12/534,526.

Morris, D., Saponas, T. S., Guillory, A., and Kelner, I. (2014). Recofit: using a wearable sensor to find, recognize, and count repetitive exercises. In *Proceedings of the SIGCHI Conference on Human Factors in Computing Systems*, pages 3225–3234. ACM.

Optitrack (2019). Optitrack flex 13 (accessed 9/17/2014).

Reiss, A., Hendeby, G., Bleser, G., and Stricker, D. (2010). Activity recognition using biomechanical model based pose estimation. In *5th European Conference on Smart Sensing and Context (EuroSSC)*, pages 42–55.

Sakurai, Y., Faloutsos, C., and Yamamuro, M. (2007). Stream monitoring under the time warping distance. In *2007 IEEE 23rd International Conference on Data Engineering*, pages 1046–1055.

Salehi, S., Bleser, G., Reiss, A., and Stricker, D. (2015). Body-imu autocalibration for inertial hip and knee joint tracking. In *Proceedings of the 10th EAI International Conference on Body Area Networks*, BodyNets '15, pages 51–57, ICST, Brussels, Belgium, Belgium. ICST (Institute for Computer Sciences, Social-Informatics and Telecommunications Engineering).

Salehi, S., Bleser, G., and Stricker, D. (2014). Design and development of low-cost smart training pants (stants). In *4th International Conference on Wireless Mobile Communication and Healthcare, At Athen, Greece*, pages 39–44. IEEE.

Seel, T., Raisch, J., and Schauer, T. (2014). Imu-based joint angle measurement for gait analysis. *Sensors*, 14(4):6891–6909.

Um, T. T., Babakeshizadeh, V., and Kulić, D. (2017). Exercise motion classification from large-scale wearable sensor data using convolutional neural networks. In *2017 IEEE/RSJ International Conference on Intelligent Robots and Systems (IROS)*, pages 2385–2390. IEEE.

Yan, X., Li, H., Li, A. R., and Zhang, H. (2017). Wearable imu-based real-time motion warning system for construction workers' musculoskeletal disorders prevention. *Automation in Construction*, 74:2–11.

Zhu, R. and Zhou, Z. (2004). A real-time articulated human motion tracking using tri-axis inertial/magnetic sensors package. *IEEE Transactions on Neural systems and rehabilitation engineering*, 12(2):295–302.

Zinnen, A., Blanke, U., and Schiele, B. (2009). An analysis of sensor-oriented vs. model-based activity recognition. In *2009 International Symposium on Wearable Computers*, pages 93–100. IEEE.